NASA TECHNICAL NOTE

PERFORMANCE CHARACTERISTICS OF A 14.3-KILOVOLT-AMPERE MODIFIED LUNDELL ALTERNATOR FOR 1200 HERTZ BRAYTON-CYCLE SPACE-POWER SYSTEM

by David S. Repas and Richard A. Edkin

Lewis Research Center
Cleveland, Ohio

PERFORMANCE CHARACTERISTICS OF A 14.3-KILOVOLT-AMPERE

MODIFIED LUNDELL ALTERNATOR FOR 1200 HERTZ

BRAYTON-CYCLE SPACE-POWER SYSTEM

By David S. Repas and Richard A. Edkin

Lewis Research Center
Cleveland, Ohio

NATIONAL AERONAUTICS AND SPACE ADMINISTRATION

ABSTRACT

The measured performance of a 14.3-kVA modified Lundell or Rice alternator is presented. Test results include alternator saturation curves, losses and efficiency, voltage unbalance, harmonic analysis, machine reactances, and time constants. The peak electromagnetic efficiency of the alternator was 93.6 percent for a unity power factor load of 9.5 kW. For an output of 14.3 kVA at 0.75 power factor lagging, the alternator electromagnetic efficiency was 90.3 percent.

PERFORMANCE CHARACTERISTICS OF A 14.3-KILOVOLT-AMPERE

MODIFIED LUNDELL ALTERNATOR FOR 1200 HERTZ BRAYTON-

CYCLE SPACE-POWER SYSTEM

by David S. Repas and Richard A. Edkin

Lewis Research Center

SUMMARY

The measured performance of a 14.3-kilovolt-ampere modified Lundell or Rice alternator is presented. Test results include alternator saturation curves, losses and efficiency, voltage unbalance, harmonic analysis, machine reactances, and time constants.

The peak electromagnetic efficiency of the alternator was 93.6 percent for a unity power factor load of 9.5 kilowatts. For an output of 14.3 kilovolt-amperes at 0.75 power factor lagging, the alternator electromagnetic efficiency was 90.3 percent.

INTRODUCTION

A single-shaft Brayton-cycle space-power system is being investigated at the NASA Lewis Research Center (refs. 1 and 2). The turbomachinery package of this power system has a compressor, a turbine, and an alternator on a high-speed shaft supported by gas bearings. The Brayton thermodynamic cycle is closed loop and uses a helium-xenon mixture as the working fluid.

One of the main objectives of present investigations of the Brayton power system is the determination of individual component performance characteristics. The purpose of this report is to present an experimental evaluation for one of these components, the alternator.

The alternator runs on gas bearings, and shaft seals are not used. Thus, the helium-xenon gas is present in the rotor cavity. Because of the high molecular weight of the gas (83.8) and the high pressure at rated load conditions, approximately 45 psia (3.10×10^5 N/m^2 abs), one of the prime considerations in the choice of the type of alternator was to minimize the windage loss to keep component efficiency high.

A brushless, stationary-coil modified Lundell alternator was chosen. Since this alternator has a smooth cylindrical rotor, it offers potentially lower windage loss than the homopolar inductor alternator that is presently being used in both the SNAP-8 (ref. 3) and 400-hertz Brayton-cycle power systems (ref. 4). A comprehensive study of the Lundell alternator for application to space-power systems is presented in reference 5.

Extensive tests were conducted at the Lewis Research Center on an experimental alternator that was designed and built primarily for obtaining alternator performance. This research package experimental alternator was designed to be electromagnetically equivalent to the alternator that will be used in the complete Brayton-cycle electrical power system. However, although gas bearings will be used in the Brayton-cycle system alternator, oil-mist-lubricated bearings were used in the experimental alternator to simplify the electrical testing.

The design, fabrication, and preliminary testing of the alternator were performed by the AiResearch Manufacturing Company, a division of the Garrett Corporation, under NASA Contract NAS 3-9427.

In this report, results of measurements of alternator saturation, efficiency, harmonic analysis, voltage unbalance, machine reactances, and time constants are presented.
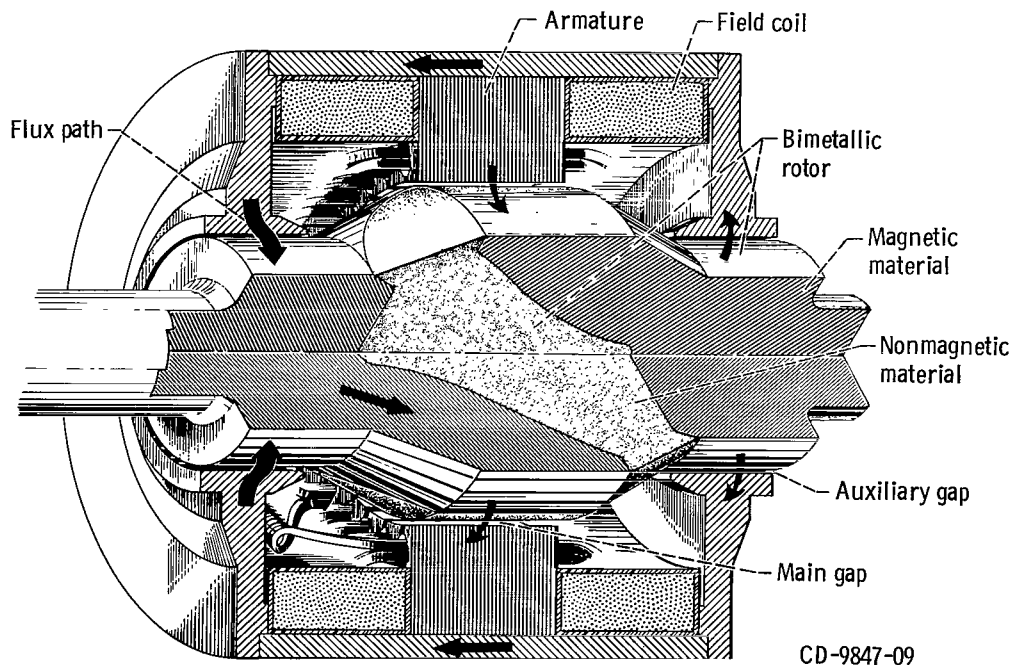

Figure 1. - Cutaway view of Lundell alternator.

DESCRIPTION OF ALTERNATOR

The alternator is a solid-rotor modified Lundell or Rice machine. It has the following continuous rating: 14.3 kilovolt-amperes, 0.75 lagging power factor, 120/208 volts, three phases, 1200 hertz at 36 000 rpm. The alternator is oil cooled.

A cutaway view of this type of Lundell alternator showing the basic configuration and flux path is presented in figure 1. The rotor of the alternator consists of two separate magnetic sections with north poles on one section and south poles on the other. The interpolar space is filled with a nonmagnetic metal to obtain a strong, smooth rotor. The main flux enters the armature stack opposite the north poles of the rotor, flows around the stack, and reenters the rotor at the south poles. The path is then completed through the auxiliary gaps, end bells, and frame. Thus, an alternating flux is established in the armature winding as in a conventional synchronous machine.

Figure 2 is a photograph of the complete assembled alternator research package. A photograph of the rotor showing the magnetic and nonmagnetic sections is presented in figure 3. Design data and features for this alternator can be found in reference 6.

One of the features that is of importance in reporting the test results is that the alternator has two windings per field coil, one for series excitation and the other for shunt
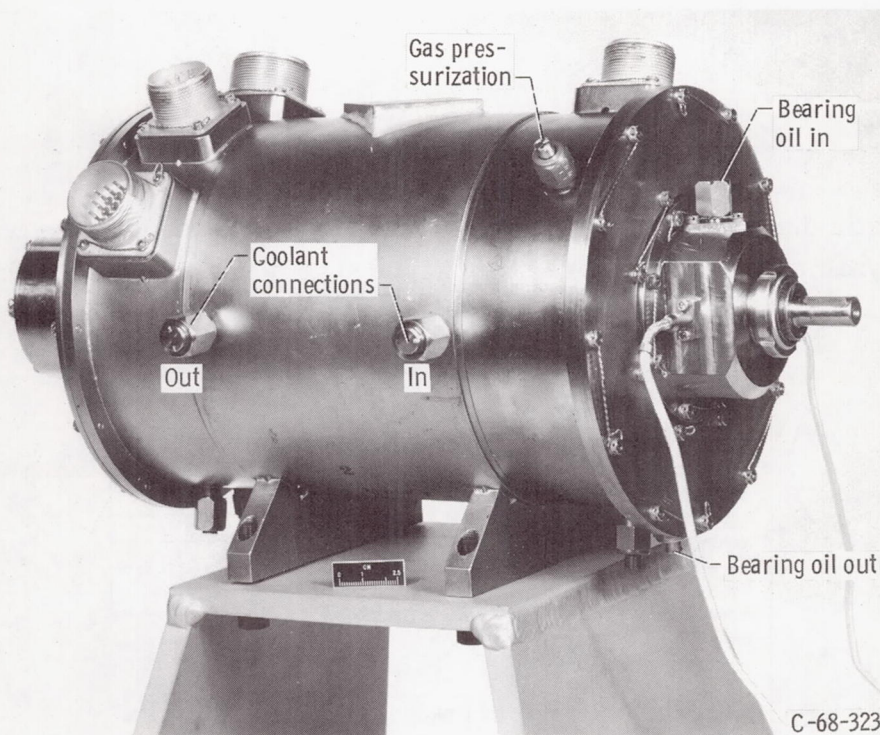

C-68-323
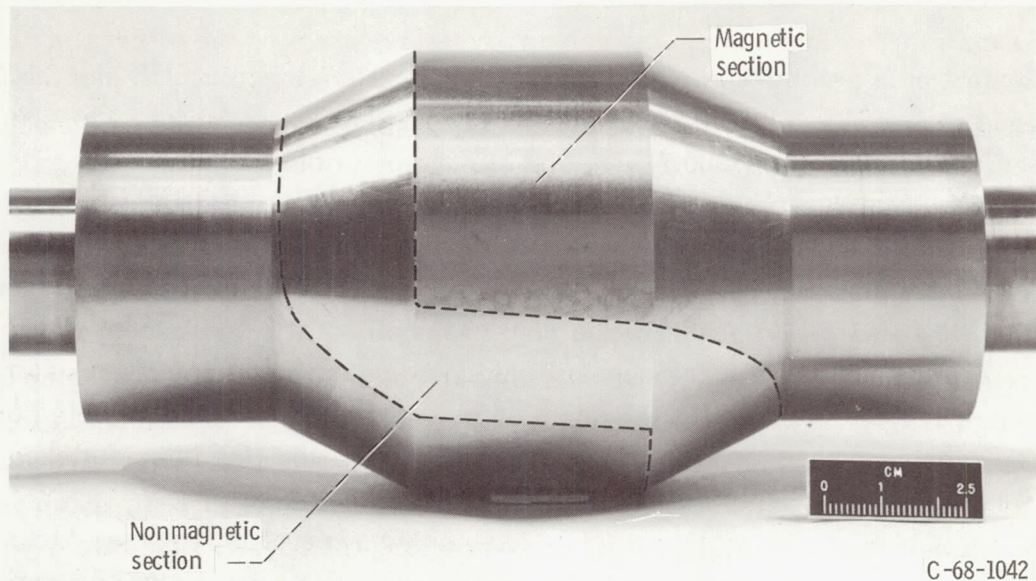
Figure 2. - Research alternator.

Figure 3. - Alternator rotor.

excitation. The series winding produces a magnetomotive force that is directly proportional to the armature current. The shunt winding produces the additional magnetomotive force required to maintain constant alternator terminal voltage.

APPARATUS AND PROCEDURE

A schematic diagram of the basic components in the test setup is shown in figure 4. A dc motor dynamometer that utilizes two stepup gear boxes was used to drive the exper-

1 Torquemeter
2 Speed meter (counter)
3 Temperature meter, pressure meter, and flowmeter
4 Voltmeter, ammeter, frequency meter, wattmeter, and oscilloscope
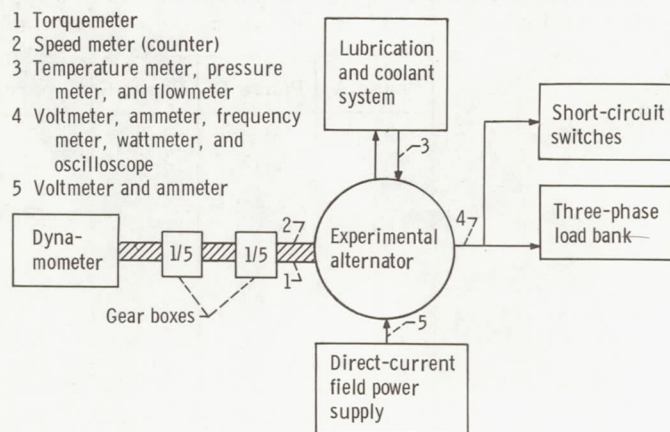5 Voltmeter and ammeter

Figure 4. - Test setup.

imental alternator at 36 000 rpm. The alternator was separately excited by a regulated dc power supply. The lubrication and coolant system controlled the alternator inlet oil (specification MIL-L-7808) temperature for each test and provided preheating capability. A three-phase load bank was used to apply resistive and reactive loads on the alternator. Short-circuit switches were used to apply three-phase faults on the machine.

Instrumentation

The positions where the instrument sensors were installed in the test setup are indicated in figure 4. The basic parameters monitored or measured included (a) shaft torque, (b) shaft speed, (c) electrical frequency, (d) terminal voltage, (e) armature current, (f) power output, (g) field current, (h) field voltage, (i) stator temperatures, (j) coolant temperature, (k) coolant inlet pressure, and (l) coolant flow rate.

Torque was measured with an electromagnetic transducer located between the alternator and drive system. A brief description, including instrument specifications, of the torque measurement system is given in the appendix. Specifications for all other instruments are given in reference 4. Prior to their use, the specific instruments required

TABLE I. - DESIGN GOALS OF BRAYTON ELECTRICAL SYSTEM

Alternator rating	14. 3 kVA at 0. 75 power factor			
Alternator efficiency	Maximized for range of 2. 25 to 10. 7 kW			
Design life	5 yr			
Harmonic distortion for linear loads (line-to-neutral voltage)	(1) Maximum individual harmonic, <3 percent for any load (2) Total harmonic content, <5 percent at 1. 0 power factor from 10 to 100 percent load (10. 7 kW)			
Voltage unbalance for 1. 0 power factor loads	Load, per unit			Maximum unbalance, percent
	Phase A	Phase B	Phase C	
	0	0	1/3	3
	0	0	2/3	6
	1/3	1/2	1/3	1. 5
	1/3	2/3	1/3	3
	1/3	1	1/3	6
	2/3	5/6	2/3	1. 5
	2/3	1	2/3	3
	5/6	1	5/6	1. 5
Overload	21. 3 kVA at 0. 75 power factor for 5 sec			

for each test were calibrated to 1 percent of full scale or better against a standard accurate to 0.25 percent.

Procedure

Table I lists the design goals of the Brayton electrical system. Unless otherwise indicated in this report, the alternator test procedure was based on approved methods described in reference 7. For all testing, alternator load power factors are lagging from zero to 1.0.

RESULTS AND DISCUSSION

Saturation

Alternator saturation curves were experimentally determined for various load conditions. For these tests, the series and shunt fields were connected in series to simplify measurement of total ampere-turns. Curves for open circuit, zero power factor, and three-phase short circuit are shown in figure 5(a). The open-circuit curve shows that a minimum combined field excitation of 1070 ampere-turns is required to generate rated terminal voltage. The zero-power-factor curve was obtained by varying the reac-
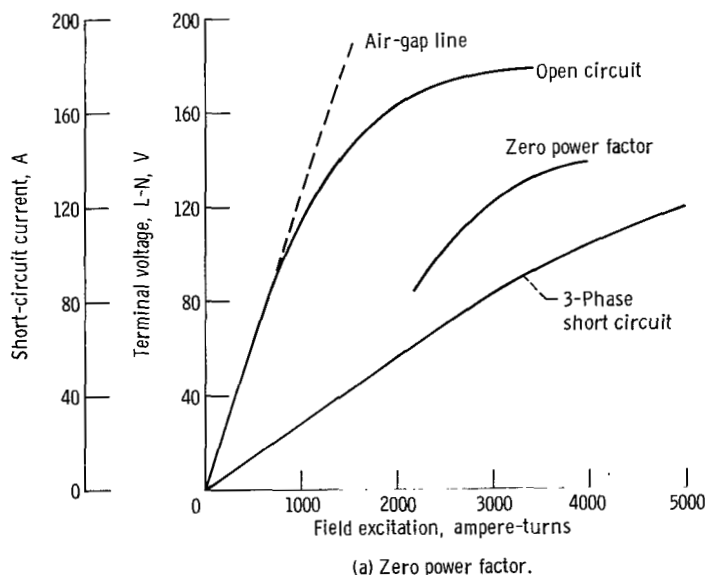
(a) Zero power factor.

Figure 5. - 1200-Hertz Lundell alternator load saturation curves.

(b) Unity power factor. Per-unit current of 1 equals 39.7 amperes.

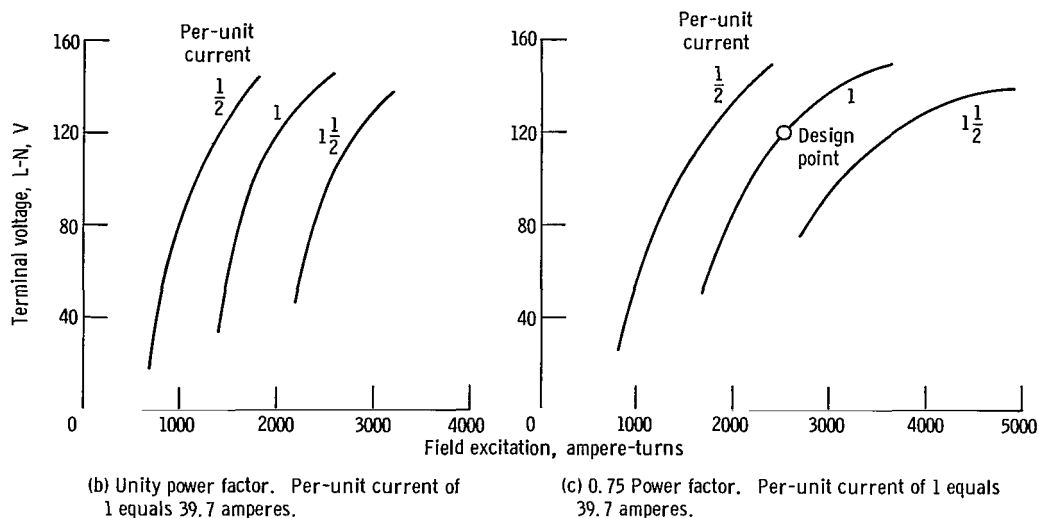(c) 0.75 Power factor. Per-unit current of 1 equals 39.7 amperes.

Figure 5. - Concluded.

tive load and increasing the field excitation to obtain rated armature current. At zero power factor, a field excitation of 2930 ampere-turns is necessary to generate rated terminal voltage.

For short-circuit saturation, a balanced three-phase fault was applied at the alternator terminals and an x, y-recording of short-circuit current (rms value) as a function of field excitation was obtained. For this test, the external lead resistance was 0.007 ohm per phase. The data indicate that the alternator can deliver 3 per unit current (119 amperes) to a balanced three-phase short circuit. However, saturation of the alternator occurs at 3 per-unit current.

Families of load saturation curves at power factors of 1.0 and 0.75 are given in figures 5(b) and (c). The curves for 0.75 power factor demonstrate that the alternator has the electromagnetic capacity to deliver rated output (14.3 kVA). The alternator also has the capability to generate 1.5 per-unit output (21.3 kVA). This output meets the overload design goal given in table I.

Losses

The following losses were individually measured so that alternator efficiency could be determined from the separation-of-losses method: (1) armature copper, (2) field copper, (3) open-circuit core, (4) stray load, and (5) windage. The measured electromagnetic losses are listed in table II for 1/4 to $1\frac{1}{4}$ per-unit output. Windage loss was ex-

TABLE II. – ELECTROMAGNETIC EFFICIENCY OF

1200-HERTZ LUNDELL ALTERNATOR[a]

[Air in cavity; cavity pressure, 14.7 psia $(1.01\times10^5$ N/m^2 abs); inlet coolant temperature, 17° C; power factor, 0.75 lagging.]
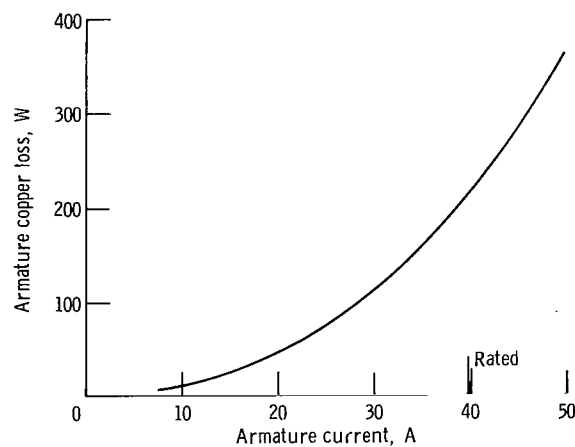
Alternator output,					
kVA	3.57	7.13	10.7	14.3	17.9
kW	2.68	5.35	8.03	10.7	13.4
Losses, kW					
Armature copper	0.011	0.045	0.109	0.214	0.362
Field copper	.021	.027	.042	.062	.096
Open-circuit core	.340	.340	.340	.340	.340
Stray load	.020	.110	.272	.530	.930
Total losses	.392	.522	.763	1.146	1.728
Electromagnetic efficiency, percent	87.2	91.1	91.3	90.3	88.6

[a]Bearing and windage losses not included.

cluded because of the uncertainty of the test results. This omission is discussed later in this section. Bearing friction is not included, because special oil-lubricated bearings were used in the experimental alternator.

Armature copper. - A curve for armature copper loss at a coolant temperature of 17° C is shown in figure 6(a). At the design temperature and rated armature current, the armature copper loss is 0.214 kilowatt.

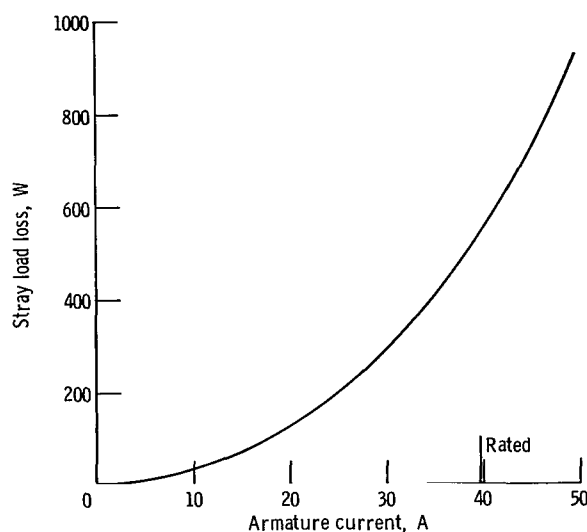Field copper. - Curves of field loss as a function of alternator power output are pre-

(a) Armature copper loss.

Figure 6. – Power losses in 1200-hertz Lundell alternator. Inlet coolant temperature, 17° C.

8
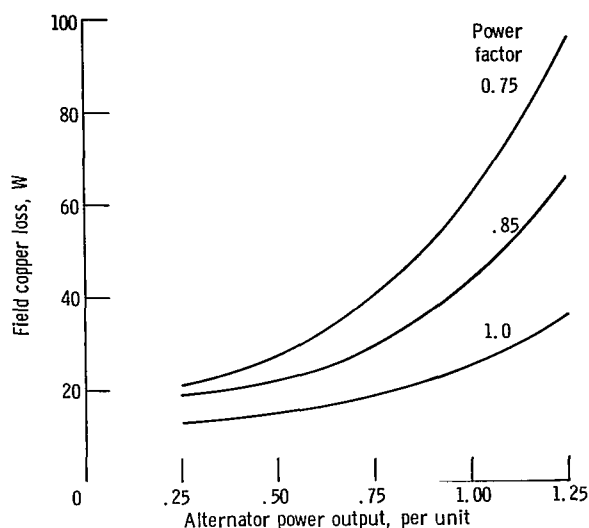
(b) Field copper loss. Output of 1 per unit equals 10.7 kilowatts.

(c) Stray load loss.

Figure 6. - Continued.

sented in figure 6(b). The losses shown are the combined total for both the shunt and series fields. At rated alternator output, the field loss was 0.062 kilowatt.

Open-circuit core. - A curve of open-circuit core loss as a function of alternator terminal voltage could not be obtained experimentally because of the limitations of the torque readout instrumentation (see appendix).

The core loss at rated voltage was determined in the following manner. With the alternator unexcited and running at rated speed, the torque meter was set to zero. Field excitation was then applied to obtain an alternator open-circuit terminal voltage of 120 volts line to neutral, and a torque reading was taken. Because of the torque instrumentation problem, this test was repeated numerous times until a consistent set of readings was obtained. For 120 volts line to neutral, the open-circuit core loss was determined to be 0.340 kilowatt.

Stray load. - Stray load loss (fig. 6(c)) was experimentally determined from a balanced 3-phase short-circuit test on the alternator. At rated load, the stray load loss was 0.530 kilowatt.

Windage. - A test was run to determine the magnitude of the alternator windage loss when a helium-xenon mixture is present in the rotor cavity. For this alternator, the windage loss is expected to be relatively high, between 6 to 10 percent of rated power output at rated load. This high loss is the result of the high molecular weight of the helium-xenon mixture and the pressure in the cavity, approximately 45 psia (3.10×10^5 N/m^2 abs), at rated alternator output.

For the test, krypton was used as the gas in the rotor cavity. Krypton has the same

9
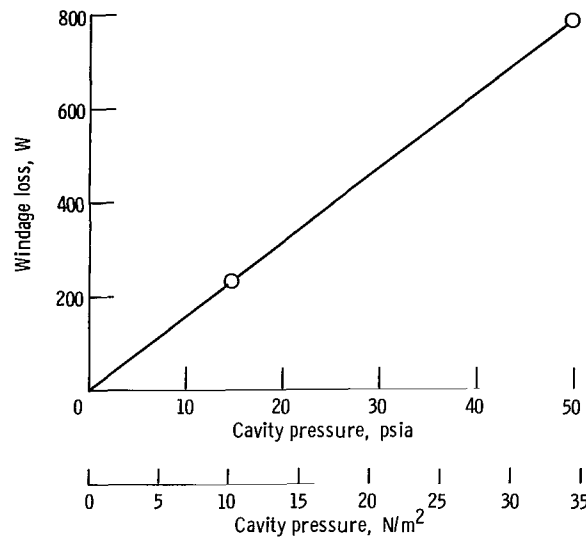
(d) Windage loss with krypton in rotor cavity.

Figure 6. - Concluded.

molecular weight of 83.8 and the same viscosity as the helium-xenon gas that will be used in the Brayton-cycle system. A load of 10.7 kilowatts at a power factor of 1.0 was connected to the alternator to stabilize the torque reading. A difference in torque was then obtained for cavity pressures of 14.7 and 49.7 psia $(1.01 \times 10^5$ and 3.43×10^5 N/m^2 abs). By assuming that the plot of windage loss against cavity pressure is linear, these data can be extrapolated back to zero pressure, which corresponds to zero windage loss. Based on this assumption, figure 6(d) was obtained.

Based on the experimental results of reference 8, figure 6(d) will probably give a low value of windage loss for a given cavity pressure. As indicated in figure 7, the theoretical curve of windage loss plotted against cavity pressure is concave downward and passes through the origin. Thus, as shown in the figure the straight-line extrapolation would intercept the zero cavity pressure axis at some finite value of windage loss.
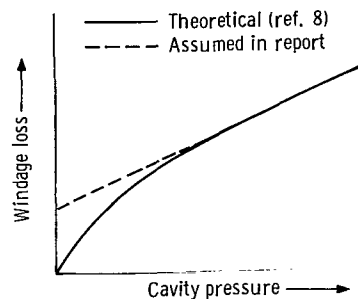

Figure 7. - Windage loss variation with cavity pressure.

By assuming that the intercept was at zero windage loss as was done to obtain figure 6(d), a low value of loss would result for a given cavity pressure.

One other unknown in the measurement of windage is the effect of cavity pressure on seal losses. A labyrinth seal is used as part of the research package system to keep the bearing oil out of the rotor cavity. The pressure drop across this seal will change as the cavity pressure is varied. This pressure drop change will probably result in a change in seal loss, which will be included in the torque readings. This change is probably small when compared with the difference in torque readings due to the windage loss. However, no data on this effect are available.

Efficiency

Alternator electromagnetic efficiency was calculated from the equation

$$\text{percent efficiency} = \frac{\text{power output}}{\text{power output + losses}} \times 100$$

Curves of electromagnetic efficiency plotted against alternator power output for various load power factors are given in figure 8. Windage and bearing losses are not included.

For rated output, the alternator electromagnetic efficiency is 90.3 percent. Over the range of 0.25 to 1.0 per-unit power output, the alternator efficiency exceeds 87 percent for power factors greater than or equal to 0.75 lagging. For a power factor of 1.0, the peak efficiency is 93.6 percent at 9.5 kilowatts (0.89 per unit).
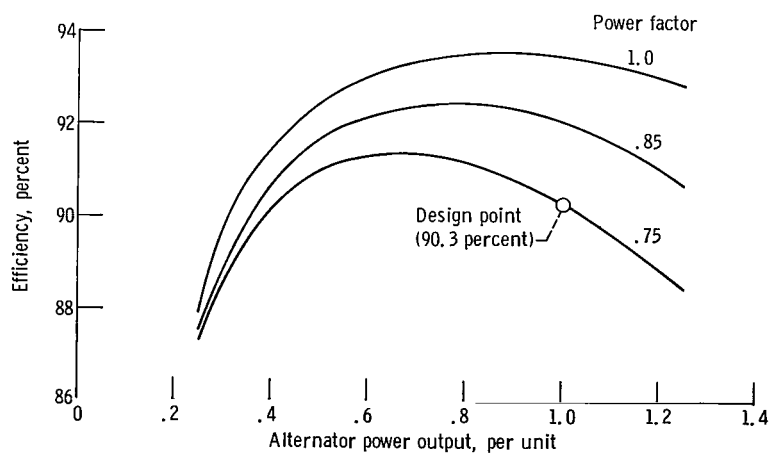
Figure 8. - 1200-Hertz Lundell alternator electromagnetic efficiency at inlet coolant temperature of 17° C. Output of 1 per unit equals 10.7 kilowatts.
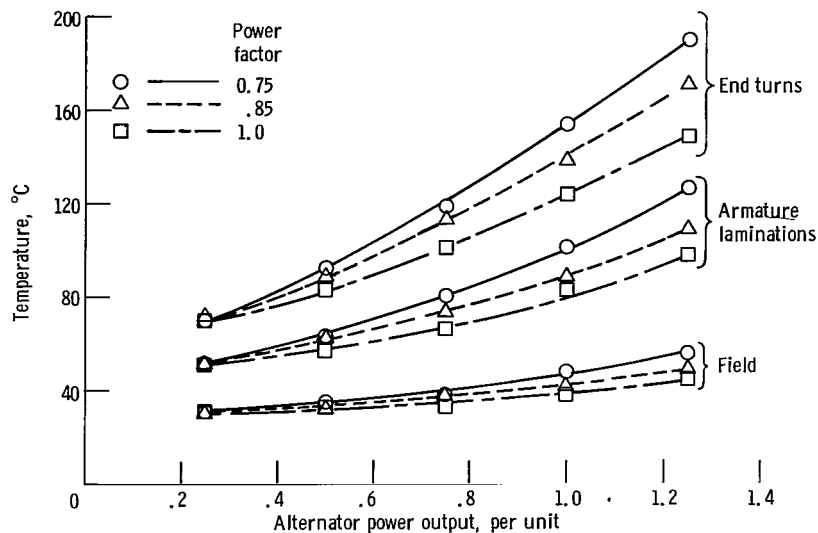
11

Figure 9. – 1200-Hertz Lundell alternator temperatures as function of load. Inlet coolant temperature, 17° C; output of 1 per unit equals 10.7 kilowatts.

Temperatures

The variation of alternator temperatures with load is shown in figure 9. These data are with air in the rotor cavity at atmospheric pressure. At the design inlet coolant temperature, the alternator has the thermal capacity to generate rated output continuously.

With air in the rotor cavity, the alternator windage loss is low in comparison with the windage loss with the higher molecular weight helium-xenon gas in the cavity. Also, at rated output of the alternator, the rotor cavity pressure with helium-xenon gas will be approximately 45 psia (3.10×10^5 N/m^2 abs) rather than atmospheric. Thus, for the Brayton-cycle system alternator, higher temperatures than those shown in figure 9 are expected because of the higher windage loss. Some idea of this increase was obtained from the krypton windage loss tests that are described in the section entitled Windage.

Table III shows a comparison of alternator temperatures with air in the rotor cavity at atmospheric pressure and with krypton in the cavity at a pressure of 49.7 psia (3.43×10^5 N/m^2 abs). The case with air can be considered to be a "zero" windage loss condition as compared with the case with krypton. For these tests, the alternator output was 10.7 kilowatts at a power factor of 1.0.

A comparison of these results shows that the end-turn temperatures increase by 37° C, and the armature lamination temperatures increase by 22° C with krypton. These increases are probably somewhat higher than would occur in the Brayton-cycle system alternator, since the rotor cavity pressure will be approximately 45 psia (3.10×10^5

12

TABLE III. – COMPARISON OF ALTERNATOR

TEMPERATURES FOR AIR AND FOR

KRYPTON IN ROTOR CAVITY[a]

	Temperature, $^\circ$C		
	Air[b]	Krypton[c]	Increase
End turns	123	160	37
Armature laminations	82	104	22
Field coil	38	38	0

[a]Alternator load, 10.7 kW at 1.0 power factor.
[b]Pressure, 14.7 psia (1.01×10^5 N/m^2 abs).
[c]Pressure, 49.7 psia (3.43×10^5 N/m^2 abs).

N/m^2 abs) rather than 49.7 psia (3.43×10^5 N/m^2 abs). Further testing is needed in this area to determine the exact effect of windage loss on the alternator temperatures.

Reactances and Time Constants

The direct-axis reactances and time constants of the alternator were experimentally determined so that the performance characteristics under transient load conditions could be predicted. They are listed in table IV.

The constants are affected by magnetic saturation and, therefore, can have either a saturated or unsaturated value. Unless otherwise specified, the test values for the

TABLE IV. – REACTANCES AND

TIME CONSTANTS[a]

Reactance, per unit[b]	
Direct-axis synchronous, X_d	1.47
Direct-axis transient, X_d'	.53
Direct-axis subtransient, X_d''	.42
Time constant, sec	
Direct-axis synchronous, T_d'	0.096
Direct-axis subtransient, T_d''	.002
Armature short circuit, T_A	.0016

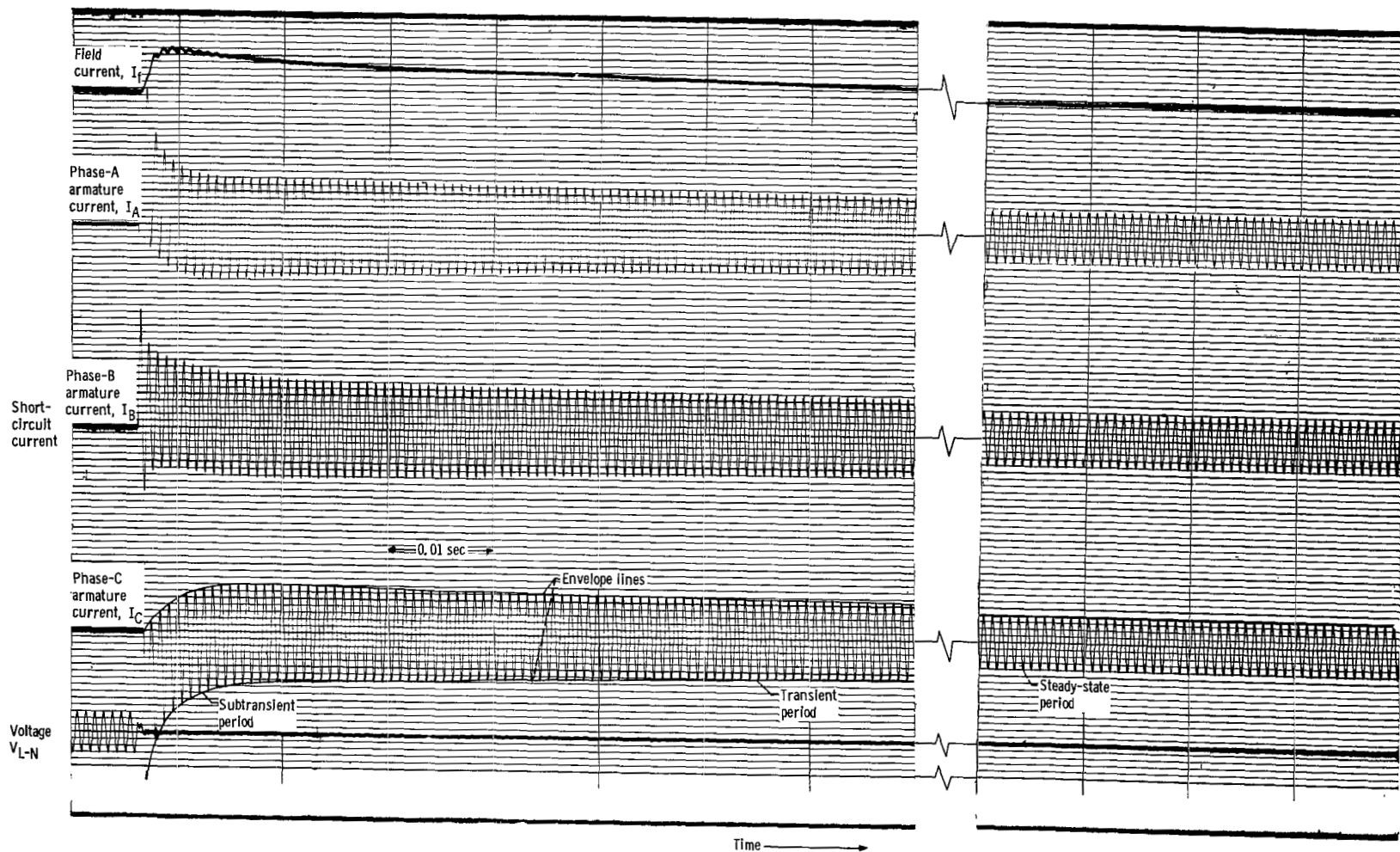[a]Test values.
[b]Base, 14.3 kVA (120 V, 39.7 A).

Figure 10. - Oscillogram of three-phase sudden short circuit.

machine constants described in this report are the saturated values. The alternator reactances and time constants were determined from a three-phase short-circuit test. In this test, the shunt field was open circuited, and only the series field was used to provide excitation. The alternator was first operated open circuit with the field excitation required to produce rated terminal voltage provided by a dc power supply. Under these conditions, a balanced three-phase short circuit was applied at the alternator terminals. The three armature phase currents and the field current were recorded on an oscillograph. An oscillogram of a three-phase short-circuit current on an alternator is shown in figure 10. The short-circuit current was analyzed for three time periods: (1) subtransient, (2) transient, and (3) steady state.

Direct-axis synchronous reactance. - Direct-axis synchronous reactance X_d can be defined as the ratio of the line-to-neutral root mean square (rms) voltage on the air-gap line (fig. 5(a)) to the armature current on a sustained three-phase short circuit for the same value of field current. In this report, the field current for rated armature current was used. The effect of armature resistance is neglected in the determination of X_d because the resistance is small in comparison with the reactance. The per-unit unsaturated value for X_d was calculated by dividing this ratio by the system base ohms, where

$$\text{base ohms} = \frac{\text{rated line-to-neutral voltage}}{\text{rated armature current}}$$

Direct-axis subtransient reactance. - The direct-axis subtransient reactance X_d'' is the reactance that determines the initial rms value of the ac component of short-circuit current that flows in the armature winding upon the application of a sudden three-phase short circuit at the alternator terminals. Figure 11(a) is a graphical analysis of the ac component of short-circuit armature current into the subtransient and transient currents. The method for obtaining the values for figure 11 is described in reference 7. The per-unit value of X_d'' was calculated from
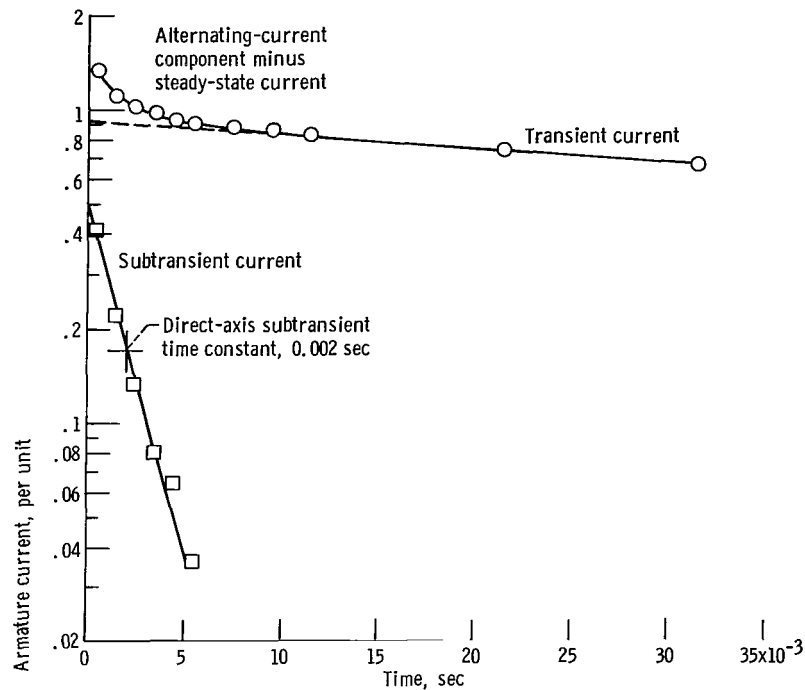
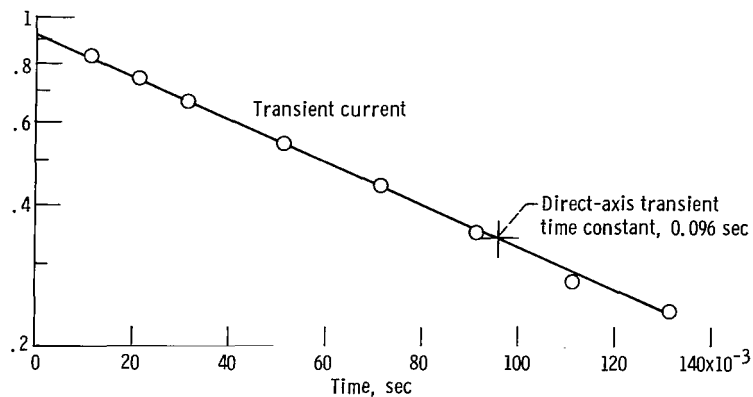$$X_d'' = \frac{E}{I''}$$

where

E   per-unit open-circuit rms terminal voltage, L - N

I''   per-unit initial ac rms short-circuit component

Direct-axis transient reactance. - The direct-axis transient reactance X_d' determines the maximum value of the rms short-circuit armature current during the transient time period (as shown in fig. 10). Figure 11(b) shows the transient current of the

15

(a) Determination of direct-axis subtransient time constant.

(b) Determination of direct-axis transient time constant.

Figure 11. - Analysis of alternating-current component of short-circuit armature current. Current of 1 per unit equals 39.7 amperes.

ac component of short circuit. The per-unit value of X'_d was calculated from

$$X'_d = \frac{E}{I'}$$

where

E   per-unit open-circuit terminal voltage, L - N

I' per-unit initial transient current plus steady-state current

Direct-axis subtransient time constant. - As illustrated in figure 11(a), the direct-axis subtransient time constant T_d'' is the time required for the subtransient ac component of short-circuit current to decrease to 36.8 percent of its initial value. The subtransient period was graphically determined by subtracting the steady-state and transient currents from the total ac component. The resulting curve is approximately linear on semilogarithmic coordinates. The experimental value for T_d'' was 0.002 second.

Direct-axis transient time constant. - The direct-axis transient time constant T_d' is the time required for the transient portion of short-circuit current to decrease to 36.8 percent of its initial value, as shown in figure 11(b). The transient period is indicated by the linear portion of the curve (fig. 11(a)), which represents the ac component minus the steady-state value. The straight line extension of the transient period to the vertical axis in figure 11(a) gives the initial value of the transient current on application of the short circuit. The direct-axis transient time constant T_d' equals 0.096 second and is long compared to T_d'' (0.002 sec).

Armature short-circuit time constant and direct-current component. - The armature short-circuit time constant T_a shown in figure 12 is defined as the time required for the direct-current component of the short-circuit current waveform to decrease ex-
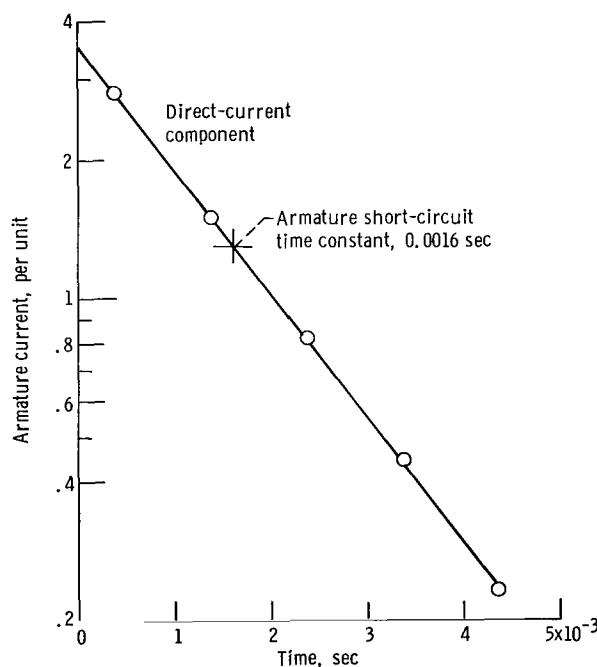

Figure 12. - 1200-Hertz Lundell alternator armature short-circuit time constant. Current of 1 per unit equals 39.7 amperes.

ponentially to 36.8 percent of its initial value. This dc component causes the current waveform to be asymmetrical, as demonstrated in figure 10.

Short-Circuit Ratio

The short-circuit ratio as determined from the saturation curves is defined by the following ratio of two values of field excitation:

$$\text{short-circuit ratio} = \frac{I_{FV}}{I_{FI}}$$

where

I_{FV} field excitation required to produce rated open-circuit terminal voltage (L - N) at rated speed

I_{FI} field excitation required for rated armature current on a sustained three-phase short circuit

These values of field excitation were determined from the open-circuit and three-phase short-circuit saturation curves in figure 5(a). The short-circuit ratio thus obtained is 0.75 for this alternator.

Voltage Unbalance

A test was conducted to determine the effects of unbalanced loads on the balance of the three-phase voltage of the alternator. The percent voltage unbalance is defined by

$$\text{percent unbalance} = \frac{\left|V_{avg} - V_{L-N}\right|_{max}}{V_{avg}} \times 100$$

where

V_{L-N} line-to-neutral voltage

V_{avg} average of three line-to-neutral voltages

Voltage unbalance results are summarized in table V. The experimental data are compared with Brayton electrical system specifications listed in table I. It is evident from the test results that the alternator meets design goals for any unity power factor load.

18

TABLE V. - VOLTAGE UNBALANCE WITH

UNBALANCED LOADS

Phase			Power factor		Maximum voltage
A	B	C	1.0	0.75	unbalance for
					1.0 power factor
Per-unit current[a]			Voltage unbalance, percent		(table I), percent
1	1	1	----	0.47	---
2/3	1	1	5.72	6.97	---
1/3	1	1	8.09	10.67	---
0	1	1	----	12.40	---
0	0	1/3	2.41	4.12	3
0	0	2/3	5.20	8.17	6
0	0	1	8.17	12.42	---
1/3	2/3	1/3	3.00	4.52	3
1/3	1	1/3	5.65	8.25	6
2/3	2/3	1	2.31	3.39	3
0	2/3	2/3	5.23	8.41	---
1/3	1/3	1/2	1.00	1.70	1.5
2/3	2/3	5/6	1.00	1.64	1.5
1	5/6	5/6	1.22	1.72	1.5

[a]1 Per-unit current equals 39.7 A.

The maximum voltage unbalance is 12.42 percent with a single-phase load at 0.75 lagging power factor and rated armature current.

Harmonic Analysis

A harmonic analysis was performed on the line-to-neutral voltage for various linear loads. (A linear load is defined as an impedance that does not change with a variation in applied voltage.)

The individual harmonics at each load condition were measured with a wave analyzer and an X, Y-recorder. Individual harmonics presented in table VI were measured in percent relative to the fundamental (100 percent). Frequencies as high as 25.2 kilohertz (21st harmonic) were measured so that the 17th and 19th slot harmonics were included.

TABLE VI. - VOLTAGE HARMONICS

FOR LINEAR LOADS

[All voltage harmonics are for line-
to-neutral voltages.]

(a) Alternator load, open circuit

Harmonic order, i	Amplitude, percent of fundamental
3	0.020
5	3.087
7	2.070
9	0
11	.755
13	1.087
15	0
17	1.850
19	2.119
21	0
Total harmonic content, percent	4.845

(b) Power factor, 1.0

Harmonic order, i	Alternator load, kW				
	2.7	5.4	8.0	10.7	13.4
	Amplitude, percent of fundamental				
3	0.283	0.603	0.880	1.077	1.272
5	3.078	2.134	1.241	1.097	1.614
7	1.862	1.397	1.225	1.269	1.223
9	.154	.190	.162	.235	.356
11	.697	.572	.343	.110	.187
13	.908	.811	.478	.185	.154
15	.077	0	.129	.199	.185
17	1.824	1.543	1.379	1.272	.982
19	1.947	1.719	1.543	1.187	1.248
21	.012	.082	.085	.051	.104
Total harmonic content, percent	4.635	3.638	2.914	2.673	2.911

TABLE VI. - Concluded. VOLTAGE HARMONICS FOR LINEAR LOADS

[All voltage harmonics are for line-to-neutral voltages.]

(c) Power factor, 0.85

Harmonic order,	Alternator load, kW				
i	2.7	5.4	8.0	10.7	13.4
	Amplitude, percent of fundamental				
3	0.255	0.548	0.778	0.980	1.110
5	3.035	2.247	1.379	.678	.731
7	1.814	1.632	1.522	1.463	1.446
9	.185	.254	.259	.257	.282
11	.603	.442	.487	.387	.381
13	.990	.972	.859	.658	.487
15	.096	.039	.015	.074	.093
17	1.799	1.538	1.087	.903	.872
19	2.183	1.945	1.911	1.781	1.594
21	.051	.060	.104	.115	.143
Total harmonic content, percent	4.686	3.920	3.273	2.866	2.766

(d) Power factor, 0.75

| Harmonic order,	Alternator load, kW				
i	2.7	5.4	8.0	10.7	13.4
	Amplitude, percent of fundamental				
3	0.237	0.476	0.752	0.831	1.049
5	3.061	2.377	1.760	1.571	1.520
7	2.093	1.737	1.620	1.597	1.474
9	.168	.254	.282	.298	.315
11	.647	.387	.453	.354	.160
13	.998	.985	.923	.849	.656
15	.093	.066	0	.036	.090
17	1.763	1.512	1.074	.949	1.057
19	2.172	2.016	1.937	1.888	1.661
21	.042	.030	.104	.121	.121
Total harmonic content, percent	4.805	4.054	3.513	3.335	3.167
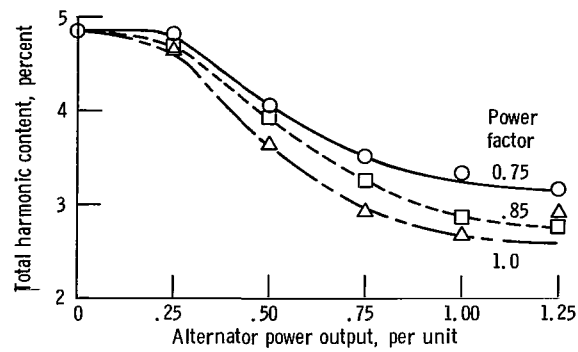
Figure 13. - 1200-Hertz Lundell alternator total harmonic content for line-to-neutral voltage. Output of 1 per unit equals 10.7 kilowatts.
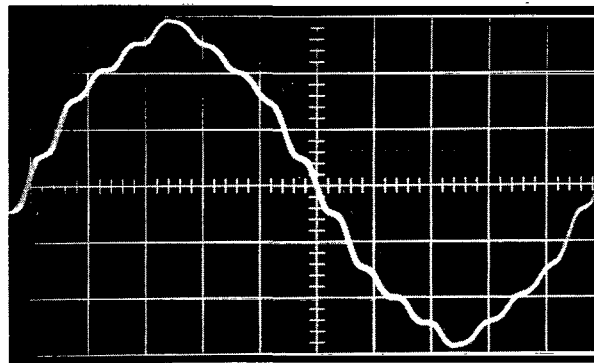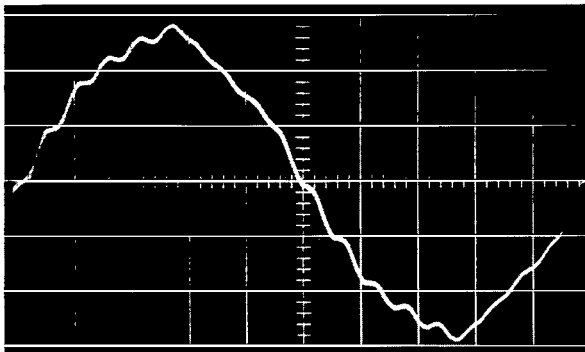

(a) Open circuit.
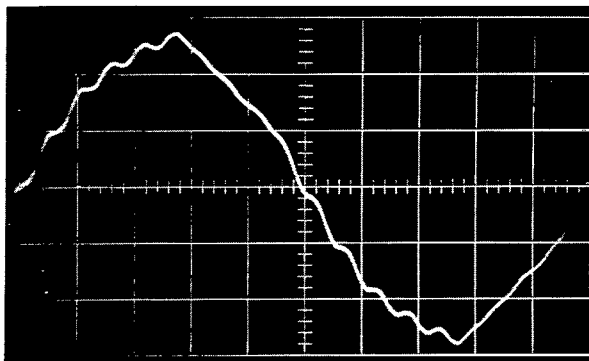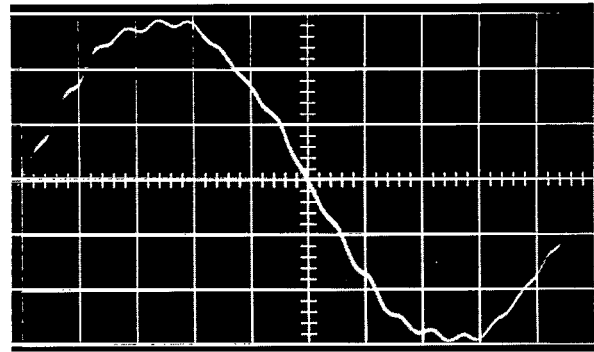

Load, 2.7 kilowatts.
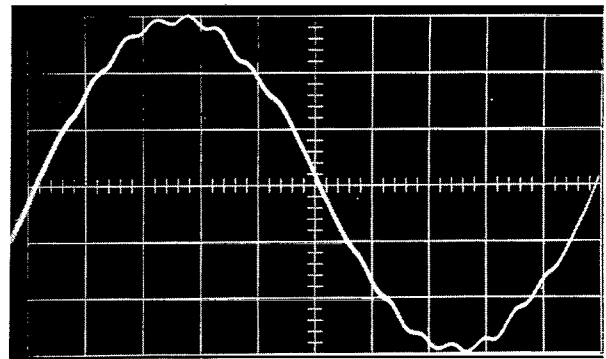
Load, 10.7 kilowatts.

(b) Unity power factor.

Figure 14. - Alternator waveforms of line-to-neutral volatges for linear loads. Uncalibrated photographs.
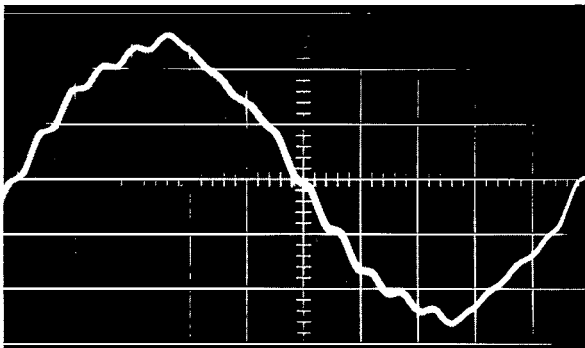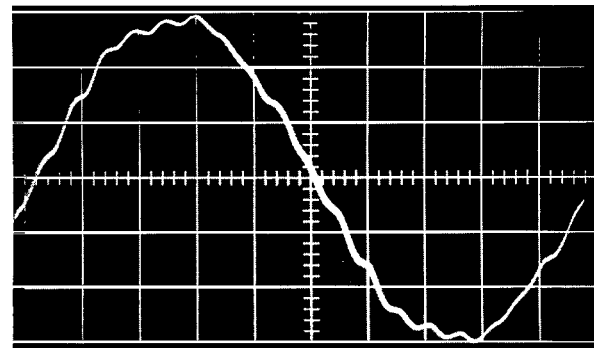
Load, 2.7 kilowatts.   (c) 0.85 Power factor.   Load, 10.7 kilowatts.

Load, 2.7 kilowatts.   Load, 10.7 kilowatts.

(d) 0.75 Power factor.

Figure 14. - Concluded.

The total harmonic content was calculated by

$$\text{percent total harmonic content} = \sqrt{\sum_{i=3}^{21} A_i^2}$$

where A_i is the percent of the ith odd harmonic relative to the fundamental. Figure 13 shows the total harmonic content as a function of alternator load.

For any of the linear loads tested, the total harmonic content is less than 5 percent and satisfies the design goal (table I). At rated kilovolt-ampere output, the line-to-neutral voltage total harmonic content is 3.34 percent. The highest individual harmonic measured was the fifth (3.09 percent) at rated voltage, open circuit. Uncalibrated photographs of the voltage wave forms are shown in figure 14 to illustrate their characteristic shapes.

SUMMARY OF RESULTS

A 14.3-kilovolt-ampere modified Lundell alternator was tested. The following significant results were obtained:

1. The alternator tested has the electromagnetic capacity to generate rated output without significant saturation. The alternator also has the electromagnetic capability to generate 1.5 per-unit output (21.3 kVA).

2. At design inlet coolant temperature, the alternator has the thermal capacity to continuously generate rated output. The exact effect of the windage loss on temperatures is uncertain.

3. For rated output of 14.3 kilovolt-amperes at 0.75 power factor, the alternator electromagnetic efficiency is 90.3 percent. For unity power factor loads, the peak efficiency is 93.6 percent at 9.5 kilowatts.

4. The total harmonic content of the line-to-neutral voltage is 3.34 percent at rated output. For the range of linear loads tested, the total harmonic content is less than 5 percent.

APPENDIX - TORQUE MEASUREMENT SYSTEM

The torque transducer used in these tests is a variable reluctance type. The torque sensor is basically a shaft that performs as a torque spring, with a slotted sleeve of magnetic material welded over the shaft. As the shaft twists under load, the air gap provided by the slot in the sleeving changes, thus causing a change in the magnetic reluctance. The change in magnetic reluctance is sensed by a variable differential transformer. The deflection of the shaft is directly proportional to the torque, and, therefore, the change in the air gap provided by the slot is directly proportional to the torque. The voltage output of the variable differential transformer is directly proportional to the change in the air gap; thus, voltage output is proportional to the torque applied.

A digital readout (two channels) is used to provide torque indication of 0 to 230 inch-pounds (0 to 25.6 N-m) with increments of 0.1 inch-pound (0.0113 N-m) from 0 to 100 inch-pounds (0 to 11.3 N-m) and increments of 1 inch-pound (0.113 N-m) from 100 to 230 inch-pounds (11.3 to 25.6 N-m). The overall accuracy is ±1/2 percent of full scale.

The torque measurement system was a state-of-the-art design at the time of the development of the dynamometer drive system. An accuracy limitation for torque readings was encountered in determining alternator losses, since at 36 000 rpm, 1 inch-pound (0.113 N-m) is equal to 427 watts.

REFERENCES

1. Klann, John L.: 2 to 10 Kilowatt Solar or Radioisotope Brayton Power System. Presented at the IEEE Intersociety Energy Conversion Engineering Conference, Boulder, Colo., Aug. 14-16, 1968.

2. Glassman, Arthur J.; and Stewart, Warner L.: A Look at the Thermodynamic Characteristics of Brayton Cycles for Space Power. Paper 63-218, AIAA, June 1963.

3. Repas, David S.; and Valgora, Martin E.: Voltage Distortion Effects of SNAP-8 Alternator Speed Controller and Alternator Performance Results. NASA TN D-4037, 1967.

4. Edkin, Richard A.; Valgora, Martin E.; and Perz, Dennis A.: Performance Characteristics of 15 kVA Homopolar Inductor Alternator for 400 Hz Brayton-Cycle Space-Power System. NASA TN D-4698, 1968.

5. Ellis, J. N.; and Collins, F. A.: Brushless Rotating Electrical Generators for Space Auxiliary Power Systems. Vol. I. Lear Siegler, Inc. (NASA CR-54320), Apr. 26, 1965.

6. Ingle, B. D.; and Corcoran, C. S.: Development of a 1200-Hertz Alternator and Controls for Space Power Systems. Presented at the IEEE Intersociety Energy Conversion Engineering Conference, Boulder, Colo., Aug. 14-16, 1968.

7. Anon.: Test Procedures for Synchronous Machines. No. 115, IEEE, Mar. 1965.

8. Vrancik, James E.: Prediction of Windage Power Loss in Alternators. NASA TN D-4849, 1968.
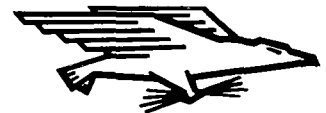
"The aeronautical and space activities of the United States shall be
conducted so as to contribute . . . to the expansion of human knowl-
edge of phenomena in the atmosphere and space. The Administration
shall provide for the widest practicable and appropriate dissemination
of information concerning its activities and the results thereof."

— NATIONAL AERONAUTICS AND SPACE ACT OF 1958

NASA SCIENTIFIC AND TECHNICAL PUBLICATIONS

TECHNICAL REPORTS: Scientific and
technical information considered important,
complete, and a lasting contribution to existing
knowledge.

TECHNICAL NOTES: Information less broad
in scope but nevertheless of importance as a
contribution to existing knowledge.

TECHNICAL MEMORANDUMS:
Information receiving limited distribution
because of preliminary data, security classifica-
tion, or other reasons.

CONTRACTOR REPORTS: Scientific and
technical information generated under a NASA
contract or grant and considered an important
contribution to existing knowledge.

TECHNICAL TRANSLATIONS: Information
published in a foreign language considered
to merit NASA distribution in English.

SPECIAL PUBLICATIONS: Information
derived from or of value to NASA activities.
Publications include conference proceedings,
monographs, data compilations, handbooks,
sourcebooks, and special bibliographies.

TECHNOLOGY UTILIZATION
PUBLICATIONS: Information on technology
used by NASA that may be of particular
interest in commercial and other non-aerospace
applications. Publications include Tech Briefs,
Technology Utilization Reports and Notes,
and Technology Surveys.

Details on the availability of these publications may be obtained from:

SCIENTIFIC AND TECHNICAL INFORMATION DIVISION

NATIONAL AERONAUTICS AND SPACE ADMINISTRATION
Washington, D.C. 20546